JACS
JOURNAL OF THE AMERICAN CHEMICAL SOCIETY

Article

pubs.acs.org/JACS

Switching Closed-Shell to Open-Shell Phenalenyl: Toward Designing Electroactive Materials

Anand Pariyar,[†] Gonela Vijaykumar,[†] Mrinal Bhunia,[†] Suman Kr. Dey,[†] Santosh K. Singh,[‡] Sreekumar Kurungot,[‡] and Swadhin K. Mandal*,[†]

[†]Department of Chemical Sciences, Indian Institute of Science Education and Research Kolkata, Mohanpur 741246, India
[‡]Physical and Materials Chemistry Division, CSIR-National Chemical Laboratory, Pune 411008, India

Supporting Information

ABSTRACT: Open-shell phenalenyl chemistry started more than half a century back, and the first solid-state phenalenyl radical was realized only 15 years ago highlighting the synthetic challenges associated in stabilizing carbon-based radical chemistry, though it has great promise as building blocks for molecular electronics and multifunctional materials. Alternatively, stable closed-shell phenalenyl has tremendous potential as it can be utilized to create an in situ open-shell state by external spin injection. In the present study, we have designed a closed-shell phenalenyl-based iron(III) complex, $Fe^{III}(PLY)_3$ (PLY-H = 9-hydroxyphenalenone) displaying an excellent electrocatalytic property as cathode material for one compartment membraneless H_2O_2 fuel cell. The power density output of $Fe^{III}(PLY)_3$ is nearly 15-fold higher than the structurally related model compound $Fe^{III}(acac)_3$ (acac = acetylacetonate) and nearly 140-fold higher than an earlier reported mononuclear Fe(III) complex, $Fe^{III}(Pc)Cl$ (Pc = pthalocyaninate), highlighting the role of switchable closed-shell phenalenyl moiety for electron-transfer process in designing electroactive materials.

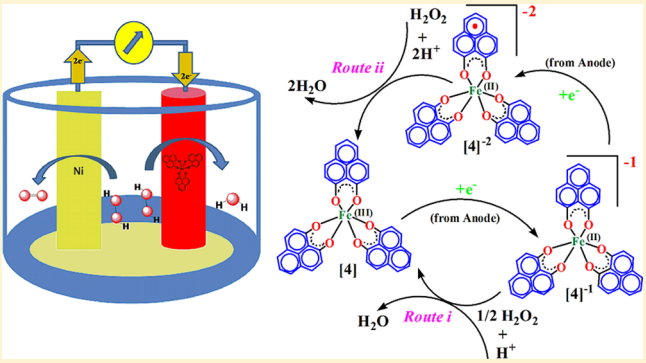

INTRODUCTION

Phenalenyl chemistry began more than half a century[1] ago, and early Hückel molecular orbital (HMO) calculations in 1960s predicted that the odd alternant hydrocarbon phenalenyl has a nonbonding molecular orbital (NBMO)[2] which can switch between closed-shell and open-shell configuration using the NBMO (Figure 1a). In the neutral state, the phenalenyl can stabilize free spin and can exist as radical using its readily available NBMO.[3] Until now, the phenalenyl chemistry predominantly relied on the open-shell (radical) state (Figure 1b). Unlike the metals, in which the unpaired electrons are largely localized, the control of quantum information and spin-based magnetic properties by chemical modification in delocalized organic radicals, such as phenalenyl, hold tremendous promise as building blocks for the construction of materials in which electron spins serve as information carriers.[4−6] Thus, the last 15 years have witnessed the evolution of a range of phenalenyl-based radicals generating an array of multifunctional materials.[7−9] Recently the use of the open-shell phenalenyl-based radical (**1**) has been extended toward designing soft organic materials for battery applications (Figure 1b).[9] The radical state of phenalenyl molecules (for example **2**, in Figure 1b) has been used as a building block to prepare intriguing materials for exploring new conjugated electronic systems, such as electronic and magnetic materials exhibiting simultaneous bistability in multiple physical channels.[7] Nevertheless, stabilizing a carbon-based radical such as the phenalenyl radical is a paramount synthetic task. It took more than two decades to realize the first phenalenyl-based neutral radical in solid state[10] since the pioneering proposal made by Haddon[3] in 1975 to utilize the NBMO of phenalenyl for construction of single component neutral radical-based conductors. This synthetic challenge of stabilizing phenalenyl-based radicals has limited the chemistry of open-shell phenalenyl to the degassed solution, Schlenk line technique, and glovebox which hindered greatly the practical utility of phenalenyl-based radicals into material application. Recent articles by Morita, Takui, and Hicks described the present status and scope of phenalenyl-based radical materials.[11,12]

Alternatively, we posed a question whether the readily available NBMO in the closed-shell electronic state (cationic state) of phenalenyl unit can be utilized to design molecular systems for novel applications. In such design, the closed-shell unit of phenalenyl can readily accept the free spin and stabilize in its NBMO, generating the open-shell state of the molecule (Figure 1a). In this design, one can synthetically avoid the unstable open-shell state but can take advantage of it by in situ generating the radical through external spin injection into the NBMO of closed-shell phenalenyl unit. Applying this principle,

Received: January 16, 2015
Published: May 1, 2015

DOI: 10.1021/jacs.5b00272
J. Am. Chem. Soc. 2015, 137, 5955−5960

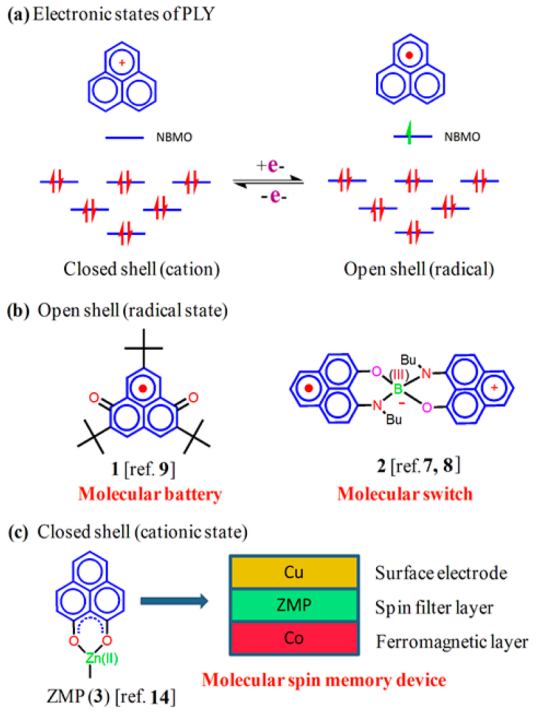

Figure 1. (a) The closed-shell and open-shell electronic states of phenalenyl that can switch through electron-transfer process using its NBMO. (b) Examples of open-shell phenalenyl-based radicals in construction of molecular battery (**1**) and bistable molecular switch (**2**) in three physical channels and (c) closed-shell (cationic state) phenalenyl-based molecule (**3**) in construction of molecular spin memory device.

we recently demonstrated the potential of the cationic phenalenyl moiety, which can be generated by metal ion coordination[13,14] with enormous potential in molecular spintronics.[14] Recently, we established that an organometallic zinc phenalenyl complex (**3**) with closed-shell phenalenyl unit on deposition over a ferromagnetic substrate readily induces spin injection to the radical state and acts as molecular spin memory device (Figure 1c).[14] This phenomena of phenalenyl moiety in the organozinc compound **3** introduces a novel molecular platform to develop a spin memory device which acts with its inherent capability of electron acceptance in the empty NBMO of closed-shell phenalenyl unit. In our endeavor to find novel properties attributed to the closed-shell phenalenyl, we present herein the use of phenalenyl moiety which can switch between closed-shell and open-shell states by electron-transfer process leading to design of electroactive materials (for cathode) in one compartment hydrogen peroxide (H_2O_2) fuel cell. The one compartment H_2O_2 fuel cell is developing as a simple, compact, efficient and environmentally benign power source.[15−17] With maximum theoretical output potential of 1.09 V, H_2O_2 fuel cell constitutes a benign alternative to fossil fuel generating H_2O and O_2 as byproducts. The H_2O_2 fuel cell operates with controlled oxidation of H_2O_2 at the anode giving O_2 and $2H^+$ ions (at 0.68 V vs NHE) and reduction of H_2O_2 at cathode producing $2H_2O$ (at 1.77 V vs NHE). Early work highlights that iron(III)-based monometallic [Fe^{III}PcCl] (Pc = pthalocyaninate) and [Fe^{III}PorCl] (Por = porphyrins) can be used as cathode materials for one compartment hydrogen peroxide fuel cell producing maximum power density of 10 μW cm^{-2}.[17] Although, the role of metal ions and their ease of access to different oxidation states are key to the electrocatalytic activity of any cathode material, the role of ligand has not yet been understood in H_2O_2 fuel cell chemistry. An appropriate understanding of auxiliary ligands' participation could be a key factor in the designing of novel materials with superior electrocatalytic properties. Therefore, we introduce phenalenyl-based molecule, 9-hydroxyphenalenone as a ligand to design the complex [$Fe^{III}(PLY)_3$](**4**) as cathode material. We also compared the power density output of **4** with $Fe^{III}(acac)_3$ (acac = acetylacetonate) and earlier reported mononuclear Fe(III) complex Fe^{III}(Pc)Cl (Pc = pthalocyaninate) revealing a significant improvement in power output for **4** (vide infra).

RESULTS AND DISCUSSION

Synthesis and Characterization. Complex **4** was synthesized by heating anhydrous $FeCl_3$ with 3 equiv 9-hydroxyphenalenone at 60 °C for 3 h in methanol to give a dark crystalline precipitate (Figure 2a). Alternatively, complex **4**

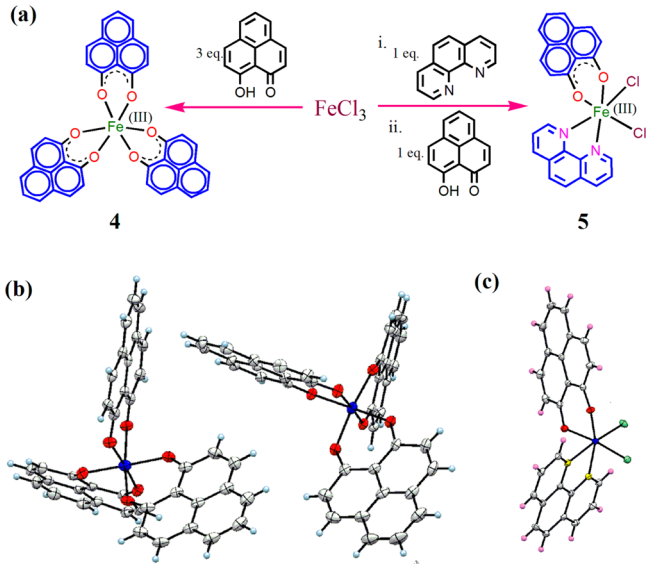

Figure 2. Synthesis and crystal structure of phenalenyl complexes **4** and **5**. (a) Synthesis of **4** and **5**. The oxidation state of iron (+3) ion is given in the parentheses, and a possible represenation of molecular drawing of **4** is discussed in Supporting Information in comparison with earlier literature[18] (see Figure S1 for details). (b) ORTEP diagrams showing asymmetric unit of **4** with two isomeric Λ and Δ units and (c) asymmetric unit of **5** with 50% probability. Solvent molecules (DMSO for **4** and acetone for **5**) are removed for the sake of clarity.

can also be prepared by solvo-thermal route heating 1:3 mixture of $Fe(NO_3)_3{\cdot}6H_2O$ and 9-hydroxyphenalenone at 120 °C for 6 h (see Supporting Information). On the other hand, the mixed ligand complex iron(III) [Fe^{III}(Phen)(PLY)Cl_2](**5**) was also designed as a control with only one phenalenyl ligand and was synthesized by reacting equimolar amount of ligands, i.e., phenanthroline, followed by 9-hydroxyphenalenone, to a stirred solution of $FeCl_3$ in acetone (see Experimental Section for details). Dark crystalline compound **5** with greenish luster was formed by keeping the reaction mixture at 4 °C. The iron(III) complexes **4** and **5** were characterized by elemental analysis, ESI-MS, EPR, IR, and single crystal X-ray diffraction studies. Single crystals of octahedral iron(III) tris-chelate complex **4** and mixed ligand complex **5** were grown in DMSO and acetone, respectively (see Supporting Information for crystallographic

DOI: 10.1021/jacs.5b00272
J. Am. Chem. Soc. 2015, 137, 5955−5960

details). The ORTEP diagram (Figure 2b) shows that the asymmetric unit of **4** consists of two isomeric units (Λ and Δ form) of octahedral iron(III) ion coordinated to three phenalenone ligands. The X-band solid-state EPR spectrum of **4** shows broad absorbance at g = 4.52 and 2.34, typical of high-spin iron(III) center (S = 5/2),[17,19] which was further confirmed by magnetic susceptibility measurements (μ_{eff} = 5.7 μ_B) at room temperature (Figures S2−S3).

Electrocatalytic Reduction of H_2O_2. The complex **4** was subsequently coated on the surface of a glassy carbon electrode (see Experimental Section for details), and the electrocatalytic reduction of H_2O_2 was evaluated. The cyclic voltammetry (CV) of H_2O_2 (3 mM) in acetate buffer (pH 3.2) using a glassy carbon (GC) electrode modified with iron(III)-complex **4** as working electrode (Figure 3a) shows a large cathodic current

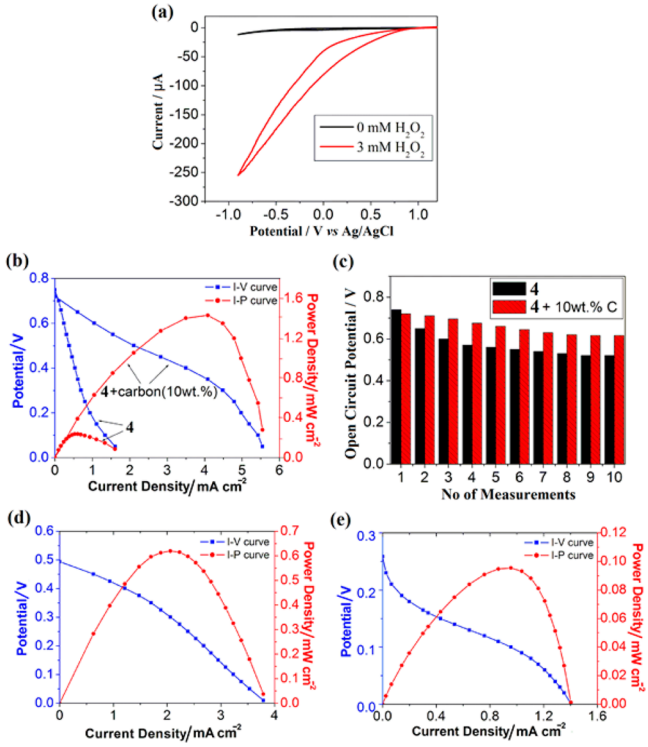

Figure 3. Electrocatalytic activity of phenalenyl-based molecules. (a) Cyclic voltammograms of H_2O_2 using GC electrode modified with **4** (pH 3.2) as working electrode, Ag/AgCl as reference, and Pt-wire as counter electrode at a scan rate of 50 mV s^{-1}. (b) Performance test of the single compartment H_2O_2 fuel cell showing I−V (blue) and I−P (red) curves using GC electrode modified with **4** +10 wt % carbon as cathode and Ni anode. (c) The change in open-circuit potential on repetitive measurements. (d) and (e) I−V (blue) and I−P (red) curves of a one-compartment H_2O_2 fuel cell with Ni anode and GC modified with (d) **5** + 10 wt % carbon and (e) $Fe^{III}(acac)_3$ + 10 wt % carbon as cathodes. Performance tests were conducted using 300 mM H_2O_2 with scan rate of 10 mV s^{-1}. Current and power were normalized by the geometric surface area of an electrode.

with an onset potential of +0.65 V (vs Ag/AgCl). The CV (Figure 3a, black curve) in absence of H_2O_2 in acetate buffer (pH 3.2) using GC electrode modified with **4** provided as background. The CV of 3 mM H_2O_2 using GC electrode without any **4** was measured as reference. Under identical condition, concurrent observations were noted with 0.1 M H_2SO_4 and 0.1 M $HClO_4$ as electrolytes (Figure S4) with the onset potential in the range of 0.15 V in acetate buffer (pH 3.2). These preliminary results indicate that **4** has excellent electrocatalytic property, which may be attributed to the controlled H_2O_2 reduction and better electron-transfer property using complex **4**. The CV of H_2O_2 (at pH 3.2) using Ni foam as the working electrode (Figure S5) shows only H_2O_2 oxidation with onset potential at 0.05 V which is much lower than that of the H_2O_2 reduction accomplished by the electrode modified with iron(III) complex **4.** This implies that the oxidation of H_2O_2 by Ni anode and reduction of H_2O_2 by **4** modified cathode would produce electric power.

One Compartment Fuel Cell Performance Test. The performance test of H_2O_2 fuel cell was carried out using an electrode modified with **4** as cathode and Ni as anode (see Experimental Section for details) with 300 mM H_2O_2 in aqueous 0.1 M H_2SO_4 (Figure 3b) and 0.1 M $HClO_4$ solutions (Figure S6a). The open-circuit potential of H_2O_2 fuel cells with **4** in 0.1 M H_2SO_4 was found to be 0.74 V, and the maximum power density reached 0.27 mW cm^{-2}. The power acquired with **4** is nearly 30-fold more than that found with $Fe^{III}(Pc)Cl$ (10 μWcm^{-2}) constructed in an identical way, and the open-circuit voltage (OCV) attained (0.74 V) is higher than that operating under basic condition (0.15 V).[16] Although thermodynamics favored the present molecular system to achieve OCV as high as 0.74 V, power density was still underyielded, and assuming that conductivity could be the retarding reason, identical experiments were performed by mixing 10 wt % of carbon in **4** to increase the conductivity. The results show almost 5-fold increase, enabling the power density to reach up to 1.43 mW cm^{-2} for **4**. Increase in carbon loading to 20 and 30 wt % did not further improve the power output. Furthermore, with 10 wt % of carbon in **4**, a sample analysis of 10 consecutive experiments showed OCV values change from 0.74 to 0.6 V (Figure 3c), which is below 20% decrease from its original value, and a relatively higher decrease (∼35%) was noticed without carbon. This implies that the stability of the H_2O_2 fuel cell with 10 wt % of carbon in **4** increases as compared to that without any carbon loading. Identical studies with **5** were also performed. The OCV using **5** as the cathode material was measured as 0.53 V, and a power density of 0.24 mW cm^{-2} was achieved. The power density showed a 2-fold increment reaching a maximum of 0.61 mW cm^{-2} when mixed with 10 wt % of carbon in **5** (Figure 3d).

In order to check the effect of phenalenyl ligand on the electrocatalytic activity of iron(III) complex **4**, identical study was performed on a PLY free complex, $Fe^{III}(acac)_3$(**6**) [acac = acetylacetonate]. $Fe^{III}(acac)_3$ was chosen as a model compound of $Fe^{III}(PLY)_3$ (**4**) containing redox inactive acetylacetonate ligand. Moreover, complex **6** is structurally similar to **4** where the phenalenyl moiety is replaced by three acetylacetonate ligands. Under identical conditions, the best result on **6** + 10 wt % carbon provides an OCV of only 0.25 V and a maximum power density of 0.089 mW cm^{-2} (Figure 3e). This value is significantly lower by nearly 15-fold as compared to the power output obtained using the iron(III) PLY complex **4**. In this regard, we note that earlier Yamada et al. reported an OCV of 0.5 V and maximum power density of 10 μW cm^{-2} at pH 3 using $Fe^{III}(Pc)Cl$ (Pc = pthalocyaninate), whereas iron(III) porphyrin complexes were found to generate an OCV of 0.125 V and maximum power density of <0.03 μW cm^{-2}.[17] Under identical conditions, the maximum power density with **4** was found to be 0.27 mW cm^{-2}, and the value is 27 times higher than that reported for the mononuclear $Fe^{III}(Pc)Cl$ complex (10 μW cm^{-2}). Further, we improved this maximum power

DOI: 10.1021/jacs.5b00272
J. Am. Chem. Soc. 2015, 137, 5955−5960

density of **4** by adding 10 wt % carbon to 1.43 mW cm^{-2}, which is 143 times higher than the most efficient neutral mononuclear Fe(III) complex reported.[17] This result clearly suggests that the phenalenyl moiety plays a key role in determining the final power output of the iron(III) complex. Also this observation points out a strong participation of the phenalenyl as a redox-active ligand in the electrocatalytic process. The iron(III) complex **4** thus evolved as the most effective monometallic Fe(III) molecule showing excellent electrocatalytic property for use in the H_2O_2 fuel cell.

CV, DFT Studies, and Mechanistic Understanding. Further, we carried out cyclic voltammetric experiments to understand the electron-transfer process operating within **4** (Figure 4).

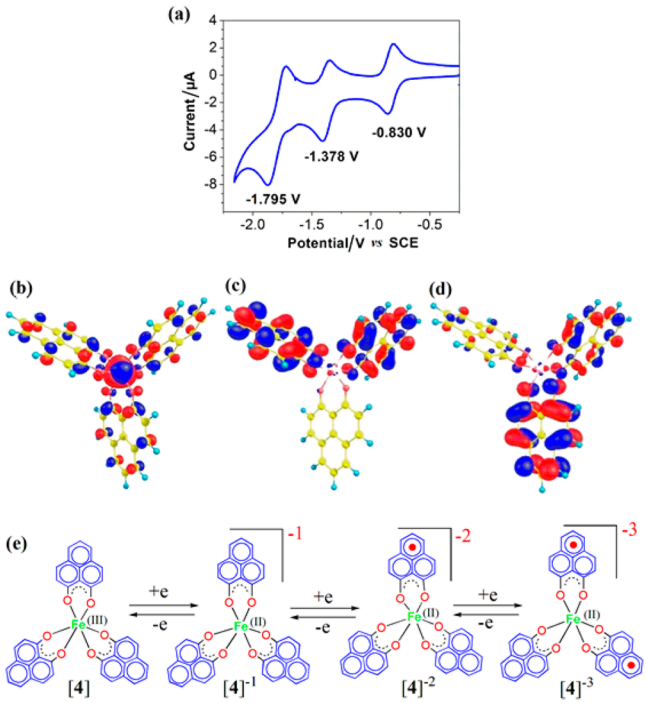

Figure 4. Electrochemical behavior of complex 4. (a) CV of **4** in DMF at a scan rate of 0.1 V s^{-1} acquired using Pt working electrode, Pt-wire as the counter electrode and reference electrode, internally referenced to ferrocene (Fc)/ferrocenium (Fc+). No oxidation signal was seen in anodic sweep up to 2 V. Isodensity plot (0.03 au) of (b) β-LUMO of **4**, (c) β-LUMO of $\mathbf{4}^{-1}$, and (d) β-LUMO+1 of $\mathbf{4}^{-1}$. (e) Three successive one electron reductions showing the formation of phenalenyl-centered radical anions. The oxidation state of iron is given in the parentheses.

On the cathodic sweep, reversible one electron reduction at $E_1^{1/2}$ = −0.83 V was observed followed by two quasi-reversible reductions at $E_2^{1/2}$ = −1.38 V and $E_3^{1/2}$= −1.79 V (vs SCE) (Figure 4a). It is to be noted that the model compound $Fe^{III}(acac)_3$ (**6**) shows reversible single electron iron(III)/iron(II) couple at $E_0^{1/2}$= −0.74 V (vs SCE)[20] which indicates that the first reduction of **4** at $E_1^{1/2}$ = −0.83 V is a predominantly metal-centered reduction to generate $\mathbf{4}^{-1}$. For further insight into the reduction process, we carried out unrestricted DFT (UB3LYP/6-311+G(d,p)) calculations[21] on **4** (see Experimental Section for details) which shows that the electron density on the β-LUMO has appreciable metal contribution (~70%, Figure 4b). This indicates that the first reduction of **4** to $\mathbf{4}^{-1}$ is predominantly metal centered. However, appreciable ligand participation cannot be completely excluded, as DFT calculations reveal that the β-LUMO of **4** has ~30% ligand contribution. This is further supported by the reported electrochemistry data of similar tris-PLY chelated molecules, $[Si(PLY)_3]^+TFPB^-$ and $[Ge(PLY)_3]^+TFPB^-$ (TFPB = tetrafluorophenylborate) compounds which exhibited three one-electron phenalenyl-centered reduction at $E_1^{1/2}$ = −0.57 V, $E_2^{1/2}$ = −0.81 V, $E_3^{1/2}$ = −1.13 V and $E_1^{1/2}$ = −0.56 V, $E_2^{1/2}$ = −0.78 V, $E_3^{1/2}$ = −1.06 V, respectively.[22] Furthermore, the electron density in β-LUMO (Figure 4c) and β-LUMO+1 (Figure 4d) of $\mathbf{4}^{-1}$ is completely based on phenalenyl moiety, which indicates that the second ($\mathbf{4}^{-1}$ to $\mathbf{4}^{-2}$, $E_2^{1/2}$ = −1.38 V) and third ($\mathbf{4}^{-2}$ to $\mathbf{4}^{-3}$, $E_3^{1/2}$ = −1.79 V) reductions of **4** are exclusively phenalenyl-based (Figure 4e) creating open-shell states of phenalenyl ligand.

Corroborating the above experimental and DFT findings, the electrocatalytic activity of **4** in H_2O_2 reduction may be understood by considering Figure 5. As established earlier,[15−17]

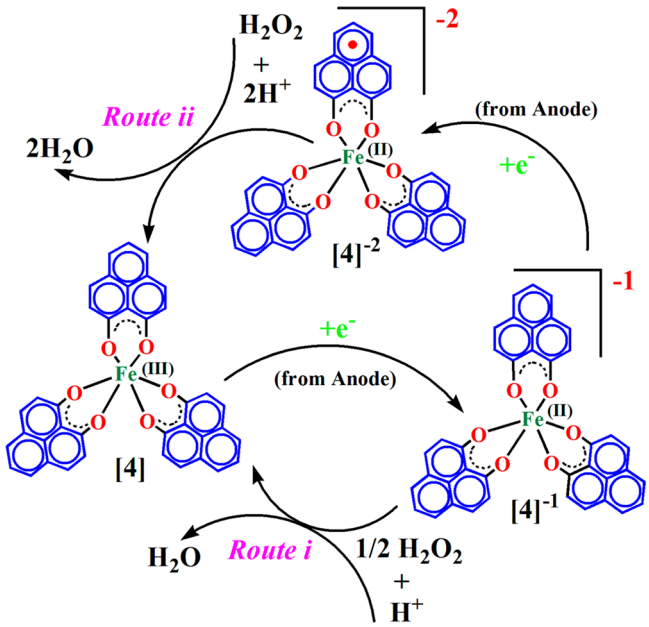

Figure 5. Plausible routes for electrocatalytic reduction of H_2O_2 using **4**. The oxidation state of iron atom is given in the parentheses.

oxidation of H_2O_2 at the anode produces electrons and H^+ ions which move toward the cathode. The produced electrons, driven by high potential (open-circuit potential) between the electrodes, subsequently move through the circuit to reach **4** and get reduced to $\mathbf{4}^{-1}$. The complex $\mathbf{4}^{-1}$ transfers electrons to H_2O_2 which in combination with diffused H^+ ions produce H_2O (*route i*) and can regenerate the catalyst **4**.

As H_2O_2 reduction is a two-electron process, the reduction depicted in *route i* considers two one-electron reduction events where two molecules of $\mathbf{4}^{-1}$ will be required. Thus, *route i* can be considered as a general one to any Fe(III)-based molecules which is based on Fe(III)/Fe(II) oxidation−reduction process and the model compound $Fe^{III}(acac)_3$ (**6**) functions following this route. Alternatively, one-step two-electron reduction of H_2O_2 can be considered, as shown in *route ii* involving two-electron reduced species $\mathbf{4}^{-2}$ as supported by our CV and DFT results. The *route ii* can work only through the open-shell state of the ligand which is possible in case of complex **4**. Therefore, during the catalytic cycle, the molecule **4** with closed-shell state

DOI: 10.1021/jacs.5b00272
J. Am. Chem. Soc. 2015, 137, 5955−5960

of phenalenyl can switch to the open-shell state (4^{-2}) by accepting two electrons. Further, 4^{-2} can take part in the H_2O_2 reduction process by transferring two electrons and regenerating **4** back through *route ii*. Thus, **4** can operate through both *routes i* and *ii* in synergy, which can remarkably influence the performance of H_2O_2 fuel cell.

CONCLUSIONS

Although open-shell chemistry of phenalenyl is already well established, the other possible electronic state, i.e., closed-shell, has not been explored to its potential, and this study is a step forward toward this direction. To the best of our knowledge, this is the first report where a redox-active ligand has been used to modulate the electrocatalytic activity of iron(III) center for H_2O_2 fuel cell application. The power density output of $Fe^{III}(PLY)_3$ in comparison to the $Fe^{III}(acac)_3$ and earlier reported mononuclear Fe(III) complex, $Fe^{III}(Pc)Cl$ (Pc = pthalocyaninate), is nearly 15- and 140-fold higher, respectively. This was atttributed to the readily available switchable electronic states of phenalenyl-based molecule in which the closed-shell phenalenyl accepts and stabilizes the free electron-generating in situ open-shell state, and then the open-shell phenalenyl can transfer the electrons for reduction of H_2O_2, regenerating the closed-shell configuration. This initial work shows that there lies an ample scope in exploring the phenalenyl-based molecules in designing cathode materials.

EXPERIMENTAL SECTION

Methods. The ligand 9-hydroxyphenalenone was prepared following the literature method.[23] Solid-state EPR analyses were done in Bruker X-band with 9.155 GHz microwave frequency, 100 kHz modulation frequency, 5 mW power, and 4 min of sweep time. The HR-MS data were obtained using a Q-Tof Micromass, Waters, instrument. Elemental analyses were performed in a PerkinElmer 2400, Series II, CHNS/O analyzer. FT-IR spectra were recorded by transmission measurements of thin film with a PerkinElmer FT-IR spectrometer Spectrum RXI. UV−vis spectroscopy was carried out with Varian Cary UV-300 spectrophotometer. X-ray crystallographic diffraction data for **4** and **5** were collected at 100 K on a SuperNova, Dual, Cu at zero, Eos diffractometer. Crystallographic data for structural analysis of **4** and **5** are deposited at the Cambridge Crystallographic Data Center, CCDC, no. 1029101 and 1029102, respectively. Copies of this information can be obtained from the Director, CCDC, 12 Union Road, Cambridge CB2 1EZ, U.K. (fax: +44 1233 336033, email: deposit@ccdc.ac.uk or www.ccdc.cam.ac.uk). All theoretical calculations were performed using the Gaussian 09 program.[24] DFT calculation employed the B3LYP functional using all electron basis sets. The geometry was fully optimized without symmetry constraints. All the atoms are treated with double-ζ quality (DZVP) basis sets of 6-311G* quality.[25]

Synthesis of $Fe^{III}(PLY)_3$ (4). To a hot solution of 9-hydroxyphenalenone (0.98 g; 5.0 mmol) in MeOH (50 mL), anhydrous $FeCl_3$ (0.27 g ; 0.16 mmol) in methanol (10 mL) was added slowly over 2 min. The color of the solution immediately turned dark-red. The reaction was refluxed for 3 h and was kept stirring for another 48 h. A thick crystalline precipitate was formed, and the solution was filtered to collect the insoluble residue. The residue was washed with methanol followed by hexane (5 times), collected, and vacuum-dried. X-ray quality crystals were grown via slow evaporation from saturated solution of DMSO. Yield: 0.45 g (43%). ESI-MS: m/z 663.64 $[M + Na]^+$. Analytically calcd for $C_{39}H_{21}FeO_6$: C: 73.03, H: 3.30; found: C: 72.92, H: 3.66. UV−vis (THF) λ_{max}/nm (ε in M^{-1} cm^{-1}): 374(36500), 428(15100), 438(15450), 455(16600), 485(14490). FT-IR(thin film) ν(cm^{-1}): 3357, 1593, 1260, 748.

Synthesis of $[Fe^{III}(Phen)(PLY)Cl_2]$ (5). $FeCl_3$ (0.081 g; 0.5 mmol) was dissolved in acetone (5 mL), and to this stirred solution, 1,10-phenanthroline (0.098 g; 0.5 mmol) dissolved in acetone (10 mL) was added. Immediately orange precipitate was observed, and to this 9-hydroxyphenalenone (0.098 g; 0.5 mmol) dissolved in acetone (10 mL) was added rapidly. The solution was vigorously stirred at room temperature for 20 h. The solution was then filtered to remove the precipitates, and the red filtrate was kept for crystallization in refrigerator at 4 °C, which yielded dark rhombic crystals in a week suitable for single crystal diffraction. The crystals were collected, washed with cold dichloromethane, and stored in vacuum. Yield: 0.13 g (52%). ESI-MS: m/z 432.11 $[M\text{-}2Cl+H]^+$. Analytically calcd for $C_{25}H_{15}Cl_2FeN_2O_2$: C: 59.50, H: 3.01; Found: C: 59.89, H: 3.07. UV−vis (THF) λ_{max}/nm (ε in $M^{-1}cm^{-1}$): 268(35320), 320^{sh}(11183), 357(10010), 494(1634). FT-IR(thin film) ν-(cm^{-1}): 3442, 1613, 1256, 1097, 750.

Electrochemical Reduction of Hydrogen Peroxide and Fuel Cell Performance Test. A small portion (10.0 μL) from isopropanol dispersion of either $[Fe(PLY)_3]$ (**4**) (1.24 mM), $[Fe(Phen)(PLY)Cl_2]$ (**5**) (2.58 mM), or $[Fe(acac)_3]$ (**6**) (1.40 mM) was drop cast on a glassy carbon electrode (surface area = 0.0707 cm^2), followed by 2 μL of nafion solution, and dried at 70 °C. The carbon mixed sample was prepared by grinding 10% (wt/wt) carbon black with iron complexes in a motor pastle using *N*-methylpyrrolidine. The finely grounded sample (10.0 μL) was then mounted on a glassy carbon electrode followed by 2 μL nafion solution. The electrochemical behaviors of H_2O_2 at electrodes modified with iron(III) complexes were examined using PAR potentiostat/galvanostat Model 263A electrochemical system. Ag/AgCl and platinum electrodes were used as reference and counter electrodes, respectively. Glassy carbon electrodes mounted with **4**, **5**, and **6** are used as working electrodes. Fuel cell performance test was performed in Biologic Science Instrument with rotating ring disk electrode (RRDE)-3A system using EC-Lab V 10.23 software. An optimum rotating speed of 900 rpm was fixed for collected data. The glassy carbon electrode modified with **4**, **5**, and **6** and Ni-foam (as anode) were immersed in a 300 mM H_2O_2 solution with aqueous solution of acetate buffer (pH 3.2), 0.1 M H_2SO_4, and 0.1 M $HClO_4$ as electrolyte. The power densities derived are within the error limit of ±0.02 mW cm^{-2}.

ASSOCIATED CONTENT

Supporting Information

Experimental details, synthesis of complexes, design and development of cathode materials, fuel cell study details, text, tables, figures, and CIF files giving details about the experiments and DFT calculations as well as X-ray structural details and a brief discussion. The Supporting Information is available free of charge on the ACS Publications website at DOI: 10.1021/jacs.5b00272.

AUTHOR INFORMATION

Corresponding Author

*swadhin.mandal@iiserkol.ac.in

DOI: 10.1021/jacs.5b00272
J. Am. Chem. Soc. 2015, 137, 5955−5960

Notes

The authors declare no competing financial interest.

■ ACKNOWLEDGMENTS

This work is dedicated to Professor S. S. Krishnamurthy on the occasion of his 75th birth anniversary. Authors sincerely thank the anonymous reviewers for their constructive suggestions in preparing the revised version of this manuscript. Authors are highly grateful to Dr. Ayan Datta for helpful discussion. A.P. thanks SERB (DST), G.V. and M.B. thank UGC-India for research fellowships. Funding from SERB (DST), India grant no.SR/S1/IC- 25/2012.

■ REFERENCES

(1) Reid, D. H. *Tetrahedron* **1958**, *3*, 339−352.
(2) (a) Reid, D. H. *Q. Rev., Chem. Soc.* **1965**, *19*, 274−302. (b) O'Connor, G. D.; Troy, T. P.; Roberts, D. A.; Chalyavi, N.; Fückel, B.; Crossley, M. J.; Nauta, K.; Stanton, J. F.; Schmidt, T. W. *J. Am. Chem. Soc.* **2011**, *133*, 14554−14557.
(3) Haddon, R. C. *Nature* **1975**, *256*, 394−396.
(4) Sato, K.; Nakazawa, S.; Rahimi, R.; Ise, T.; Nishida, S.; Yoshino, T.; Mori, N.; Toyota, K.; Shiomi, D.; Yakiyama, Y.; Morita, Y.; Kitagawa, M.; Nakasuji, K.; Nakahara, M.; Hara, H.; Carl, P.; Höfer, P.; Takui, T. *J. Mater. Chem.* **2009**, *19*, 3739−3754.
(5) Rahimi, R.; Sato, K.; Furukawa, K.; Toyota, K.; Shiomi, D.; Nakamura, T.; Kitagawa, M.; Takui, T. *Int. J. Quantum Info.* **2005**, *3*, 197−204.
(6) Nakazawa, S.; Nishida, S.; Ise, T.; Yoshino, T.; Mori, N.; Rahimi, R. D.; Sato, K.; Morita, Y.; Toyota, K.; Shiomi, D.; Kitagawa, M.; Hara, H.; Carl, P.; Höfer, P.; Takui, T. *Angew. Chem., Int. Ed.* **2012**, *51*, 9860−9864.
(7) Itkis, M. E.; Chi, X.; Cordes, A. W.; Haddon, R. C. *Science* **2002**, *296*, 1443−1445.
(8) Pal, S. K.; Itkis, M. E.; Tham, F. S.; Reed, R. W.; Oakley, R. T.; Haddon, R. C. *Science* **2005**, *309*, 281−284.
(9) Morita, Y.; Nishida, S.; Murata, T.; Moriguchi, M.; Ueda, A.; Satoh, M.; Arifuku, K.; Sato, K.; Takui, T. *Nat. Mater.* **2011**, *10*, 947−951.
(10) Goto, K.; Kubo, T.; Yamamoto, K.; Nakasuji, K.; Sato, K.; Shiomi, D.; Takui, T.; Kubota, M.; Kobayashi, T.; Yakusi, K.; Ouyanget, J. *J. Am. Chem. Soc.* **1999**, *121*, 1619−1620.
(11) Morita, Y.; Suzuki, S.; Sato, K.; Takui, T. *Nat. Chem.* **2011**, *3*, 197−204.
(12) Hicks, R. G. *Nat. Chem.* **2011**, *3*, 189−191.
(13) Sen, T. K.; Mukherjee, A.; Modak, A.; Ghorai, P. K.; Kratzert, D.; Granitzka, M.; Stalke, D.; Mandal, S. K. *Chem.—Eur. J.* **2012**, *18*, 54−58.
(14) Raman, K. V.; Kamerbeek, A. M.; Mukherjee, A.; Atodiresei, N.; Sen, T. K.; Lazic, P.; Caciuc, V.; Michel, R.; Stalke, D.; Mandal, S. K.; Blugel, S.; Munzenberg, M.; Moodera, J. S. *Nature* **2013**, *493*, 509−513.
(15) Yamazaki, S.; Siroma, Z.; Senoh, H.; Ioroi, T.; Fujiwara, N.; Yasuda, K. *J. Power Sources* **2008**, *178*, 20−25.
(16) Yamada, Y.; Fukunishi, Y.; Yamazakib, S.; Fukuzumi, S. *Chem. Commun.* **2010**, *46*, 7334−7336.
(17) Yamada, Y.; Yoshida, S.; Honda, T.; Fukuzumi, S. *Energy Environ. Sci.* **2011**, *4*, 2822−2825.
(18) Chi, X.; Itkis, M. E.; Patrick, B. O.; Barclay, T. M.; Reed, R. W.; Oakley, R. T.; Cordes, A. W.; Haddon, R. C. *J. Am. Chem. Soc.* **1999**, *121*, 10395−10402.
(19) Yamada, Y.; Yoneda, M.; Fukuzumi, S. *Inorg. Chem.* **2014**, *53*, 1272−1274.
(20) Pacześniak, T.; Błoniarz, P.; Rydel, K.; Sobkowiak, A. *Electroanalysis* **2007**, *19*, 945−951.
(21) Considering metal-centred reduction, high-spin (hs) Fe(III) in **4** may get reduced to hs Fe(II) or low-spin (ls) Fe(II) abbreviated as $\mathbf{4}^{-1}$. For calculation, hsFe(II) was considered because the ground-state energy difference between **4** with lsFe(II) was found to be more than 100 KJ mol^{-1}, whereas for hsFe(II), it's <10 $KJmol^{-1}$. Spin expectation value for **4** and $\mathbf{4}^{-1}$ are $\langle S^2 \rangle$ = 8.7500 and $\langle S^2 \rangle$ = 6.004, respectively.
(22) Pal, S. K.; Itkis, M. E.; Tham, F. S.; Reed, R. W.; Oakley, R. T.; Haddon, R. *J. Am. Chem. Soc.* **2008**, *130*, 3942−3951.
(23) Haddon, R. C.; Rayford, R.; Hirani, A. M. *J. Org. Chem.* **1981**, *46*, 4587−4588.
(24) Frisch, M. J.; Trucks, G. W.; Schlegel, H. B.; Scuseria, G. E.; Robb, M. A.; Cheeseman, J. R.; Scalmani, G.; Barone, V.; Mennucci, B.; Petersson, G. A.; Nakatsuji, H.; Caricato, M.; Li, X.; Hratchian, H. P.; Izmaylov, A.; Bloino, F. J.; Zheng, G.; Sonnenberg, J. L.; Hada, M.; Ehara, M.; Toyota, K.; Fukuda, R.; Hasegawa, J.; Ishida, M.; Nakajima, T.; Honda; Kitao, Y. O.; Nakai, H.; Vreven, T.; Montgomery, J. A., Jr.; Peralta, J. E.; Ogliaro, F.; Bearpark, M.; Heyd, J. J.; Brothers, E.; Kudin, K. N.; Staroverov, V. N.; Keith, T.; Kobayashi, R.; Normand, J.; Raghavachari, K.; Rendell, A.; Burant, J. C.; Iyengar, S. S.; Tomasi, J.; Cossi, M.; Rega, N.; Millam, J. M.; Klene, M.; Knox, J. E.; Cross, J. B.; Bakken, V.; Adamo, C.; Jaramillo, J.; Gomperts, R.; Stratmann, R. E.; Yazyev, O.; Austin, A. J.; Cammi, R.; Pomelli, C.; Ochterski, J. W.; Martin, R. L.; Morokuma, K.; Zakrzewski, V. G.; Voth, G. A.; Salvador, P.; Dannenberg, J. J.; Dapprich, S.; Daniels, A. D.; Farkas, Ö.; Foresman, J. B.; Ortiz, J. V.; Cioslowski, J.; Fox, D. J. *Gaussian 09*, Revision C.01; Gaussian, Inc.: Wallingford, CT, 2010.
(25) Schäfer, A.; Horn, H.; Ahlrichs, R. *J. Chem. Phys.* **1992**, *97*, 2571−2577.

DOI: 10.1021/jacs.5b00272
J. Am. Chem. Soc. 2015, 137, 5955−5960